Evaluation of the effect of the strain rate on the compressive response of a closed-cell aluminium foam using the split Hopkinson pressure bar test

Evaluation of the effect of the strain rate on the compressive response of a closed-cell aluminium foam using the split Hopkinson pressure bar test

I. Irausquín, J.L. Pérez-Castellanos, V. Miranda, F. Teixeira-Dias

PII: S0261-3069(12)00879-5
DOI: http://dx.doi.org/10.1016/j.matdes.2012.12.050
Reference: JMAD 5028

To appear in: *Materials and Design*

Received Date: 14 August 2012
Accepted Date: 20 December 2012

Please cite this article as: Irausquín, I., Pérez-Castellanos, J.L., Miranda, V., Teixeira-Dias, F., Evaluation of the effect of the strain rate on the compressive response of a closed-cell aluminium foam using the split Hopkinson pressure bar test, *Materials and Design* (2012), doi: http://dx.doi.org/10.1016/j.matdes.2012.12.050

Evaluation of the effect of the strain rate on the compressive response of a closed-cell aluminium foam using the split Hopkinson pressure bar test

I. Irausquín[a,b*], J.L. Pérez-Castellanos[a], V. Miranda[c], F. Teixeira-Dias[c]

[a] *Department of Continuum Mechanics and Structural Analysis, Universidad Carlos III de Madrid, Leganés 28911, Spain*
[b] *Department of Industrial Technology, Universidad Simón Bolívar, AP 89000, Caracas 1080, Venezuela*
[c] *GRIDS-DAPS-Division of Armour & Protection Systems, Dept. Mechanical Engineering, Universidade de Aveiro, 3810-193 Aveiro, Portugal*
[*] Corresponding author. Tel: +58 212 9069226; E-mail: irausqui@usb.ve

Abstract

The research here presented is focused on the evaluation of the dynamic behaviour of a closed-cell aluminium foam using the split Hopkinson pressure bar (SHPB) test. On a first approach, the influence of the material of the bars was studied and, as a consequence, polymethylmethacrylate (PMMA) was chosen as the most suitable material to be used in the bars and striker to test the specific aluminium foam considered. This set of bars was manufactured and several dynamic compression tests were carried out. The corresponding stress-strain behaviour was obtained and the dependence of mechanical parameters of the aluminium foam Alporas 10% on the strain rate was thoroughly analysed. It was possible to conclude that the material exhibits significant strain rate sensitivity, within the tested range of strain rates. The range of strain rate values where the compressive behaviour of the foam is different was also determined.

Keywords: Metallic foams, strain rate, split Hopkinson pressure bar

1. Introduction

Most metal foams are low-density cellular materials with interesting and distinct physical, mechanical, thermal, electrical and acoustic properties. Due to their high capability to absorb energy at low and constant stresses, these materials are highly indicated to be used in structural applications and impact energy absorption systems and devices [1-3]. The behaviour of metal foams has been

thoroughly investigated, mostly in *quasi*-static conditions. It is also possible to find some work done on the dynamic behaviour of metallic foams, mostly using Hopkinson bar devices [4]. However, these analyses are not always clear, and sometimes even contradictory, in relation to the possible influence of the strain rate on the mechanical response of the material.

Mechanical impedance of the materials of the bars and specimens (the product between the material density and the wave propagation speed) is a determinant parameter in terms of assuring the SHPB test validity. If the product of the mechanical impedance of specimen material to the specimen cross section is much lower than the product of mechanical impedance of bars material to the specimen bars section, the reflected and incident waves will be very similar and, consequently, the amplitude of the transmitted wave will be small and difficult to detect and register. Just like many other soft materials, metallic foams have very low mechanical impedance making it difficult to test them using a conventional SHPB apparatus, often manufactured with steel bars. To study the behaviour of low impedance materials it is then necessary to use low impedance bars. To make things even more complex, very few purely elastic materials have low impedance. PMMA and Nylon are interesting options for this particular purpose. The main problem is that these two materials have viscous behaviour, making it difficult to interpret the waves recorded during the tests.

Propagation of waves in viscoelastic bars is prone to attenuation and dispersion, even if geometrical effects are not significant, so that, different methods have been developed to correct their effects on such a kind of materials [5-11].

Concerning the dynamic behaviour of the metallic foams, several studies have been done not always with coherent results in terms of their sensitivity to strain rate. Deshpande and Fleck [12] tested Alulight and Duocel foams using PMMA bars and determined that both materials were strain rate sensible up to 5000 s^{-1}. On a different work by Dannemann and Lankford [13], it was verified that Alporas foams with relative densities of 7.4 and 15% exhibit some degree of strain rate sensitivity. Nonetheless, the small size of the specimens used by these authors compared with the foam cell size

probably induces some dispersion in the results. Zhao *et al*. [14] on their work on the strain rate sensitivity of aluminium foams, used Nylon bars and corrected the wave dispersion (due to the viscoelastic behaviour of the bars) using the Pochhammer-Chree solution. On a systematic work, Tan *et al*. [15] performed direct impact tests on steel bars to investigate the dynamic behaviour of the Cymat aluminium foam observing some strain rate sensitivity on the plastic collapse stress but not on the plateau stress. Zhao *et al*. [16] analysed the behaviour of IFAM aluminium foams under direct impact using Nylon bars and corrected the dispersion of the waves using the Pochhammer-Chree theory. Tan *et al*. [15] verified that this foam did not show significant strain rate sensitivity. However, later Mukai *et al*. [17] used a Hopkinson bar to test Alporas aluminium foam samples and observed that the material exhibits some degree of strain rate sensitivity, most evident on the elastic limit (considered to be the maximum peak stress value on the stress-strain plot). Nonetheless, two aspects of the tests done by Mukai *et al*. [17] can affect the quality of the results: the small size of the specimens (inducing cell size effects) and the authors used steel bars with inappropriate mechanical impedance for the material being tested. Additionally, these authors did not implement any type of correction for the dispersion and determined the stress in the material comparing one, two and three waves. Later work on IFAM foams by Peroni *et al*. [18] used aluminium alloy bars and showed no strain rate sensitivity. More recently, Kiernan *et al*. [19] used Nylon bars to compress Alporas foam samples and determined that there is some degree of strain rate sensitivity on the plateau stress region. However, these same authors recognise that some of the samples they used were not representative due to their small size.

The main goal of the present work is to characterise the dynamic behaviour of an Alporas metallic foam using the SHPB test. For this purpose, a SHPB apparatus using viscoelastic PMMA bars was designed, manufactured and calibrated. Several tests of the foam were performed using this device at different strain rates. The dynamic elastic modulus of the material was determined using the ultrasonic inspection procedure. Nominal stress-strain curves were derived from the recorded waves once the effect of viscoelastic dispersion and attenuation was corrected using a numerical/experimental

procedure proposed by Bacon [9]. From these curves were obtained the mechanical parameters of the foam and its sensitivity to the strain rate was analysed.

2. Experimental device: The split Hopkinson pressure bar (SHPB)

2.1. SHPB description

A schematic and generic representation of a Hopkinson compression test apparatus is shown in Fig. 1.

When the compression pulse and the incident wave generated from the impact of the striker against the input bar reach the bar-specimen interface, it separates into a reflected tensile wave which travels along the input bar and a compression transmitted wave which travels along the output bar.

The three deformation pulses, incident (ε_i), reflected (ε_r) and transmitted (ε_t) are recorded using the strain gauges on the bars. The dynamic equilibrium of the specimen – necessary condition for the validity of the test – can be checked by forcing the loads (F) on the input bar-specimen and specimen-output bar interfaces, that is,

$$F_{input}(t) = AE\left[\varepsilon_i(t) + \varepsilon_r(t)\right], \tag{1}$$

$$F_{output}(t) = AE\varepsilon_t(t), \tag{2}$$

to be equal. In these expressions A and E are both the cross section area and the Young's modulus of the bars, respectively.

2.2. Analysis of the recorded waves

According to the theory of one-dimensional wave propagation the waves registered by the strain gauges are the exact same waves that one would register at the interfaces because they suffer no change while propagating along the bars. This being the case, expressions (1) and (2) become equal at the strain gauges. Besides verifying the dynamic equilibrium of the specimen, the validity of such an experiment is only guaranteed if the stress state is one-dimensional and axially uniform, and the strain

field in the specimen is also uniform.

Wave dispersion and attenuation

The harmonic components that compose the waves propagating along the bars travel at different velocities and can become out of phase with each other. If the bars are made from a viscoelastic material the waves can suffer from dispersion and attenuation, leading to a mismatch between the waves recorded on the strain gauges and the waves on the bar-specimen interfaces. In order to apply expressions (1) and (2) it is then necessary to correct these viscoelastic dispersion and attenuation effects.

Considering an infinite cylindrical bar and one-dimensional axial wave propagation, the relation between phase velocity and frequency is governed, in the elastic case, by the frequency equation proposed by Pochhammer [20] and Chree [21]. Applying the Pochhammer solution it is then possible to confirm that the ratio between the actual velocity of the wave C and C_0 is a function of the ratio R/Λ between the radius of the bar, R, and the wavelength, Λ. This ratio becomes equal to 1 (i.e. $C = C_0$) when $R/\Lambda = 0$. The phase velocity, C, reduces with the increase in the frequency, w, the high-frequency components of the wave travel at lower velocities than the lower-frequency components, leading to oscillations on the rear of the wave and increasing the time it takes for the pulse to rise.

In this work was used the method developed by Bacon [7] to correct the effects of the viscoelastic dispersion and attenuation, by considering an axial impact against a cylindrical bar made from a viscoelastic material, with length L, cross section area A and density ρ. A strain gauge is positioned on a point on the bar defined as $x = 0$; the far end of the bar ($x = d$) is free (on these conditions the test is said to be "empty").

The viscoelastic behaviour of the material can be described defining the elastic modulus as a function of the frequency. The relation between the Fourier transforms of the stress and strain is then

$$\tilde{\sigma}(x,\omega) = E^*(\omega)\tilde{\varepsilon}(x,\omega) \tag{3}$$

Defining the material propagation coefficient as

$$\gamma^2(\omega) = -\frac{\rho\omega^2}{E^*(\omega)} \tag{4}$$

the solution of one-dimensional equation of axial motion is given by

$$\varepsilon(x,\omega) = \tilde{P}(\omega)e^{-\gamma x} + \tilde{N}(\omega)e^{\gamma x} \tag{5}$$

where functions $\tilde{P}(\omega)$ and $\tilde{N}(\omega)$ are the Fourier transforms (FT) of the incident wave, $\varepsilon_1(t)$, and reflected wave after reflexion at the free end ($x = d$), $\varepsilon_2(t)$, registered at $x = 0$, that is,

$$\tilde{\varepsilon}_1 = \tilde{P} \quad \text{and} \quad \tilde{\varepsilon}_2 = \tilde{N}. \tag{6}$$

The incident wave, $\varepsilon_1(t)$, and the reflected wave, $\varepsilon_2(t)$, are registered separately and the strain gauge positioned at $x = 0$.

The real and imaginary parts of $\gamma(\omega)$ are the coefficient of attenuation (or damping coefficient), $\alpha(\omega)$, and the phase number, $k(\omega)$, respectively, $k(\omega)$, can be related to the phase velocity, $C(\omega)$, through the expression

$$\gamma(\omega) = \alpha(\omega) + i\frac{\omega}{C(\omega)} = \alpha(\omega) + ik(\omega) \tag{7}$$

Consequently, and given the fact that the far end of the bar is free, the load is zero, then

$$\tilde{P}(\omega)e^{-\gamma x} + \tilde{N}(\omega)e^{\gamma x} = 0 \tag{8}$$

from where it is possible to obtain the transfer function, $H^*(\omega)$,

$$H^*(\omega) = -\frac{\tilde{\varepsilon}_2(\omega)}{\tilde{\varepsilon}_1(\omega)} = e^{-\gamma 2d} \tag{9}$$

.

From $H^*(\omega)$ it is then possible to determine the propagation coefficient, $\gamma(\omega)$, and its two components: the attenuation coefficient, $\alpha(\omega)$, and the wave number, $k(\omega)$.

Stress-strain curves determination

Consider a SHPB test where the incident, ε_i, reflected, ε_r, and transmitted, ε_t, strain waves were

recorded using strain gauges. The following expression can be used to correct these waves:

$$e^C = FFTI\left[e^{-\gamma 2d} FFT[e]\right] \tag{10}$$

where e designates the uncorrected wave and e^C the corrected wave. The acronyms FFT and FFTI designate Fast Fourier Transform and Inverse Fast Fourier Transform, respectively.

The nominal (engineering) strain, ε_N, the strain rate, $\dot{\varepsilon}_N$, and the nominal (engineering) stress, σ_N, can then be determined from the corrected reflected and transmitted waves using the expressions

$$\varepsilon_N = \frac{2C}{L_0}\int_0^t \varepsilon_r dt, \tag{11}$$

$$\dot{\varepsilon}_N = \frac{2C}{L_0}\varepsilon_r, \tag{12}$$

$$\sigma_N = E\frac{A}{A_s}\varepsilon_t, \tag{13}$$

where L_0 and A_s are the initial length and cross section area of the specimen and A is the cross section area of the bar.

2.3. Design and implementation of a viscoelastic SHPB

A specific SHPB device was designed and implemented in order to perform the dynamic compression tests on metal foam specimens. According to previous discussion, the following criteria were defined for the design of the SHPB device:

a) The bars should be made from a material with a similar mechanical impedance to the metallic foam specimens;

b) The diameter of the bars should be large enough to ensure that no dynamic buckling effect was present during the tests so that it was possible to determine the behaviour of the tested material (foam); and

c) The length of the striker should be large enough to guarantee that the incident and reflected waves were not coincident in time.

When manufacturing the bars, three different materials were considered, namely: steel, Nylon PA6 and PMMA. For comparison purposes, values of the product of the mechanical impedance, $Z = \rho C$, of these materials by the cross section area of the bar (or specimen), *A*, are listed in table 1. The same parameter was calculated for the tested Alporas foam and is also listed.

The value of ZA for the foam is 0.8% of the corresponding value for a steel bar. This fact would lead to a test where the incident wave would be almost fully reflected, not producing a transmitted wave. As a consequence, using steel bars would lead to a test where no stress values could be determined (eq. 13). However, both PMMA and Nylon PA6 have very similar values of ZA. For these materials the value of ZA of the foam is approximately 17%, leading to a transmitted wave that can be used to determine the evolution of stress on the specimen.

To confirm these initial conclusions and to choose the SHPB configuration and the bar materials, the modelling of the dynamic compression of the metal foam in accordance to the SHPB test was done elsewhere [22] using the FEM commercial code Abaqus version 6.9-2 [23]. The constitutive behaviour model chosen for the metallic foam specimen was based on the one developed by Deshpande [24]. The numerical results were used to define the overall configuration of the SHPB system. PMMA proved to be the best option among the materials considered for both the bars and striker, in terms of incident pulse shape and amplitude and attenuation of the reflected wave. Nylon could also be a reasonable option but it was discarded due to its fragility and lower hardness. Thus, PMMA bars were built with 1 m in length and 32 mm in diameter. A striker with the same diameter and 330 mm in length was also built.

The PMMA compression Hopkinson bar system developed is shown in Fig. 2a. Two optic fibre sensors were used to measure the impact velocity of the striker on the input bar, as can be seen in Fig. 2b. This velocity was determined as the ratio between the exact distance between the two sensors and the time interval the striker takes to cross them. Four strain gauges were fixed at 50 cm from each

specimen-bar contact and connected into a Wheatstone bridge; this distance was determined taking into account the length of the incident, reflected and transmitted pulses.

3. Experimental testing

3.1. Materials and test procedure

The metallic foam tested within the scope of this work was an Alporas 10%, manufactured by Shinko Wire Company, Ltd. (Japan) in liquid state using the blowing agent procedure [25] leading to a nominal chemical composition Al-1.5Ca-1.5Ti.

The density of the foam was determined and found to be $\rho^* = 265$ kg/m^3. Considering that the density of aluminium (and its alloys) is approximately equal to 2700 kg/m^3, the relative density of the foam, ρ^*/ρ_s, is then approximately equal to 0.1 (10%).

The foam from where the specimens were cut was received in 440×220 mm^2 plates with three different thicknesses: 12, 18 and 30 mm. In order to define the best dimensions for the specimens it was considered that, first at all, these must be representative of the whole cellular material. Following the work of Chen *et al*. [26,27], the height to diameter ratio was chosen between 0.5 and 1 and, consequently, cylindrical specimens having 26 mm both in height and in diameter were cut. Accepting that the average cell size of the Alporas 10% is 2.6 mm [28], the cell size effects are supposedly avoided because the specimens had at least 7 cells along its diameter.

In accordance with DYMAT standardisation RE/002B/87 [29], the interfaces between specimen and bars were lubricated to minimise friction effects and the bars were carefully aligned to avoid non-uniform strain fields. The SHPB testing and the data processing were conducted following recommendations of the aforementioned standard.

3.2. Dynamic Young's modulus measurement

To estimate the σ_N-ε_N stress-strain relations it is necessary to know the elastic modulus

(Young's modulus) of PMMA. The value of this property, made available by the manufacturer, is most certainly obtained from *quasi*-static tests. However, several authors have previously reported that this property is frequency dependent [11,30-33]. Some of these authors suggest that the dynamic elastic modulus should be measured using the ultrasonic technique due to its non-destructive character. This approach was followed in this work and the resulting elastic modulus for PMMA was compared with the value of this parameter obtained by measuring the duration of a pulse recorded in SHPB test.

The ultrasonic longitudinal wave propagation velocity (V_{uw}) in homogeneous media (such as PMMA) is a function of the elastic modulus, density and Poisson's ratio, that is,

$$V_{uw} = \sqrt{\frac{E}{\rho} \cdot \frac{1-\nu}{(1+\nu)\cdot(1-2\nu)}} \tag{14}$$

A Krautkramer USD 10 equipment was used to measure the velocity V_{uw} using the pulse-echo contact method. This method requires the use of dual transducers that act as transmitter and receiver of the ultrasonic signal. Measurements were carried out using five different transducers, leading to an average velocity of V_{uw} = 2712 ± 29 m/s.

The resulting average value of V_{uw} coincides with that determined by Afifi [34] for PMMA using the same ultrasonic test method. Consequently, the value of the Poisson's ratio of PMMA was considered the same as that reported in the referred work [33], that is ν = 0.34. Considering that the density of PMMA is ρ = 1190 kg/m^3 [35] – value confirmed by measuring the mass and volume of a cylindrical specimen – it is possible to determine that the Young's modulus is E = 5.7 GPa.

3.3. Correction procedure of the dispersion and attenuation

Experimental determination of the propagation coefficient using Bacon's method

Several tests at different impact velocities were performed to apply the method described in section 2.2, using only the input bar. The incident, ε_1, and reflected, ε_2, waves were recorded and the procedure described followed to obtain the propagation coefficient, $\gamma(\omega)$, using expression (8), and its components: the attenuation coefficient, $\alpha(\omega)$, and the phase number, $k(\omega) = \omega / C(\omega)$. The incident and reflected waves registered on an empty test performed at 1.5 bar, are shown in Fig. 3.

The obtained attenuation coefficient, $\alpha(\omega)$ is shown in Fig. 4. Although this coefficient should not be dependent on the procedure used to obtain it, some small differences were found from the results of tests at different strain rates. These differences may possibly be due to the numerical definition of both the starting point and the duration of the pulse.

Effect of the dispersion and attenuation corrections on the recorded waves

The reflected and the transmitted waves obtained on each test were corrected following the procedures described in previous paragraphs. This correction consisted in pushing the waves backwards 50 cm, corresponding to the distance the wave travels from its initiation (at the input bar-specimen interface) to where it is registered, at the strain gauge on the input bar (for the incident wave) or at the strain gauge on the output bar (for the transmitted wave).

Fig. 5 shows the incident wave and the sum of the waves reflected and transmitted, as recorded from a SHPB test at 500 s^{-1} (Fig. 5a) and as obtained once the correction procedure was applied (Fig. 5b). The correction was made using the propagation coefficient obtained from an empty test at 1.5 bar of pressure.

From Fig. 5 it is possible to conclude that the corrected waves verify the additive relation and therefore it is possible to accept that the loads on the interfaces (expressions 1 and 2) are equal, so that the specimen is in dynamic equilibrium.

Lifshitz and Leber [36] concluded on the difficulty to determine either the exact moment when the strain pulse starts or the wave velocity, from the waves recorded on SHPB tests. These authors also demonstrated that the shape of the σ_N-ε_N curves is sensible to small deviations on both parameters (pulse initiation and wave velocity). In this work were analyzed different possibilities for the initiation of the pulse and it was found that there is a limited dependence of this parameter for the tested material and impact velocity considered in the tests.

4. Results and Discussion

Within the scope of this work were performed experimental SHPB tests in which the velocity of the striker was in the range of 10 to 18 m/s, leading to strain rate values between 400 and 900 s^{-1}. A striker with 330 mm in length was used in the tests in order to ensure that the incident and reflected waves were not superimposed.

Although the internal structure of the metallic foam is heterogeneous, it was possible to observe that the strain field on the tested specimens was uniform.

Nominal stress-strain curves

The nominal stress-strain curves (σ_N-ε_N) were obtained from the corrected reflected and transmitted waves. Nominal stress-strain curves obtained with the corrected and uncorrected waves (both reflected and transmitted) are shown in Fig. 6.

Analysing the results in Fig. 6 it is possible to infer that in this case the correction leads to a small increase on the nominal stress as well as to the onset of a slight superimposed oscillation, due to the numerical definition of the wave period and of the instant when this one initiates.

The average deviation observed on the hardening region of the nominal stress-strain curves, σ_N-ε_N, for all the values of strain rate was below 10%, as can be confirmed for instance from the results shown in Fig. 7 for $\dot{\varepsilon}$ = 700 s^{-1}. The highest value of deviation was found for the higher strain rates.

This can be due to some heterogeneity on the shape, size and distribution of cells within the metallic foam specimens.

Only the first set of waves (incident, reflected and transmitted) was used to obtain these results (see Figs. 6 and 7) since the following reflections on the extremes of the bars were not numerically usable. This explains why the results are presented only for strains lower that the ones corresponding to the densification region (the corresponding strain values could only be reached for further reflected pulses).

The average σ_N-ε_N curves obtained from the dynamic tests are shown in Fig. 8 and compared to the results from *quasi*-static testing. The corresponding impact velocity, V_{st}, is indicated for each curve in the figure. From these results it is possible to observe that, as expected for ductile materials [18,19,37], the maximum strains ($\varepsilon_{N_{\max}}$) reached for the tested impact velocities are lower than that imposed for *quasi*-static testing. It can also be observed that for strain rates ranging from 500 s^{-1} to 900 s^{-1} the σ_N-ε_N curves are above the *quasi*-static curve, which makes evident the influence of this parameter. The results obtained at 400 s^{-1} do not exhibit the same tendency. This insensitivity of the σ_N-ε_N curve to the strain rate at 400 s^{-1} is probably due to internal reflexions of the impact wave within the metallic foam structure [15].

Mechanical parameters

The σ_N-ε_N curves plotted in Fig. 8 shown that for a given value of strain any increase of the strain rate (i.e. increasing the impact velocity V_{st}) leads to an increase of the corresponding stress. Fig. 9 shows the stress-strain rate relation, σ_N-$\dot{\varepsilon}$, for nominal strains between 0.05 and 0.15. The shape of these curves seems to be bilinear (or quadratic) with a decreasing slope. This particular behaviour can be associated to the microinertial effects within the foam structure that are known to cause a softening of the foam particularly effective during the early stages of the σ_N-ε_N curve [38]. The microinertial effects of the cell walls on the mechanical strength of the metallic foams have been previously studied

by authors like Deshpande and Fleck [12], Tan *et al*. [15], Zhao *et al*. [16], Paul and Ramamurty [38], and have been mainly attributed to a change in the failure mechanism of the cell walls at high strain rates.

The dynamic compression strength and plateau stress of the Alporas 10% foam was estimated from the σ_N-ε_N results. The compression strength, σ_c, was measured from the limit compression stress, which is the initial peak stress of the σ_N-ε_N curve. This property is related to the initiation of the plastic collapse of a band of cells, at a particular strain denoted as ε_c. The plateau stress, σ_{pl}, was determined as the average nominal stress value, σ_N, of the σ_N-ε_N curve, between ε_c and $\varepsilon_{N_{\max}}$. Values obtained for σ_c and σ_{pl} are plotted in Fig. 10 as a function of the strain rate. These mechanical parameters were normalised with the *quasi*-static nominal stress $\sigma_N^{0.001/s}$. The plateau stress, σ_{pl}, was normalised considering the *quasi*-static value as the average nominal stress up to a nominal strain matching $\varepsilon_{N_{\max}}$ reached in the dynamic test. Both σ_c and σ_{pl} exhibit a bilinear (or quadratic) dependence with the strain rate, which is consistent with the observations made from the analysis of the curves in Fig. 9. This dependency is in agreement with that reported by Tan *et al*. [15] for a closed-cell Hydro/Cymat aluminium foam.

The results in Fig. 10 show increments of the compression strength and the plateau stress at 500 s^{-1} that are close to the limit value of 20% in deviation proposed by Deshpande and Fleck [12] (considered as the maximum allowable deviation), whereas for strain rates higher than 700 s^{-1}, these mechanical properties exhibit an increment significantly larger than the reference deviation, so that they put in evidence a strain rate sensitivity similar to the one found on the aforementioned study.

Considering that the trapped gas in the cells has a negligible influence on the stiffness and strength of the foam [12,15] and that the base material of the cell walls has no significant strain rate dependence, the increment on the mechanical properties of the Alporas 10% foam can be attributed to microinertial effects within the structure of the foam.

Energy absorption capability

Variation of the specific absorbed energy (energy absorbed per unit volume of foam material), *W*, with the strain rate, $\dot{\varepsilon}$, is shown in Fig. 11, for nominal strains, ε_N, between 0.05 and 0.15. The absorbed energy parameter was determined by calculating the area under the nominal stress-strain curve and normalising with the corresponding *quasi*-static value. As can be observed in Fig. 11, for the considered nominal strains *W* has a linear dependence with the strain rate. In addition, the $W/\dot{\varepsilon}$ slope decreases slightly when the nominal strain increases. These two observations can be justified by an increment of the plateau stress and of the microinertial hardening, respectively. Bearing in mind that the plateau stress increases with the strain rate it becomes evident that *W* should also increase with this parameter. Regarding the $W/\dot{\varepsilon}$ slope, the influence that the microinertial effects have on the hardening of the metallic foam at low strains (on the early stages of the nominal stress-strain curve) allows to predict that this slope should decrease with the increase of the strain.

It is evident in Fig. 11 that the specific absorbed energy, *W*, increases between 20 and 60% for strain rates in the range of 500 to 900 s^{-1} compared to their *quasi*-static values. This confirms sensitivity of the Alporas 10% to the strain rate within the range considered for this parameter and agrees the increase of the energy absorption capability found by Mukai *et al*. [28].

5. Conclusions

The design, manufacture and implementation of a split Hopkinson pressure bar device with bars and striker made of PMMA has shown to be suitable for the dynamic characterisation of an Alporas aluminium foam at different strain rates.

Due to the frequency dependence of the PMMA Young's modulus, it was necessary to determine a dynamic value of this parameter using the ultrasonic inspection technique.

The viscoelastic dispersion and attenuation effects evidenced on the recorded waves were

corrected, so that the nominal stress-strain curves of the aluminium foam were obtained for different strain rates.

From the obtained results it was possible to derive evolution laws to relate the dependence between the maximum compression strength of the metallic foam, its plateau stress and its energy absorption capability with the strain rate.

Acknowledgements

This work was supported by the Centre for the Development of Industrial Technology (CDTI) of Spain and the company AERNNOVA Aerospace; this financial support is gratefully acknowledged. The authors would also like to acknowledge the financial support given by the Portuguese Science and Technology Foundation (FCT – Fundação para a Ciência e a Tecnologia), through project PTDC/EME-PME/73503/2006.

References

[1] Hou S, Li Q, Long S, Yang X, Li W. Crashworthiness design for foam filled thin-wall structures. Mater Design 2009; 30:2024-2032.

[2] Rajendran R, Prem Sai K, Chandrasekar B, Gokhale A, Basu S. Preliminary investigation of aluminium foam as an energy absorber for nuclear transportation cask. Mater Design 2008; 29:1732-1739.

[3] Reglero J, Solórzano E, Rodríguez-Pérez M, De Saja J, Porras E. Design and testing of an energy absorber prototype based on aluminium foams. Mater Design 2010; 31:3568-3573.

[4] Zou L, Zhang Q, Pang B, Wu G, Jiang L, Su H. Dynamic compressive behavior of aluminum matrix syntactic foam and its multilayer structure. Mater Design 2013; 45:555-560.

[5] Zhao H, Gary G. A tridimensional analytical solution of the longitudinal wave propagation in a infinite linear viscoelastic cylindrical bar: application to experimental techniques. J Mech Phys

Solids 1995; 43(8):1335-48.

[6] Zhao H, Gary G, Klepaczco J. On the use of a viscoelastic split Hopkinson pressure bar. Int J Impact Eng 1997; 19:319-30.

[7] Bacon C. An experimental method for considering dispersion and attenuation in a viscoelastic Hopkinson bar. Exp Mech 1998; 36(4):242-9.

[8] Cheng ZQ, Crandall JR, Pilkey WD. Wave dispersion and attenuation in viscoelastic split Hopkinson pressure bar. Shock Vib 1998; 5:307-15.

[9] Bacon C. Separation of waves propagating in an elastic or viscoelastic Hopkinson pressure bar with three-dimensional effects. Int J Impact Eng 1999; 22:55-69.

[10] Bussac M, Collet P, Gary G, Othman R. An optimisation method for separating and rebuilding one-dimensional dispersive waves from multi-point measurements. Application to elastic or viscoelastic bars. J Mech Phys Solids 2002; 50:321-49.

[11] Benatar A, Rittel D, Yarin AL. Theoretical and experimental analysis of longitudinal wave propagation in cylindrical viscoelastic rods. J Mech Phys Solids 2003; 51:1413-31.

[12] Deshpande V, Fleck N. High strain-rate compressive behaviour of aluminium alloy foams. Int J Impact Eng 2000; 24:277-98.

[13] Dannemann K, Lankford J. High strain-rate compression of closed-cell aluminium foams. Mater Sci Eng 2000; A293:157-64.

[14] Zhao H, Abdennadher S, Banhart J. An experimental study of the deformation rate sensitivity of PM aluminium foams. In: Banhart J, Fleck N, Mortensen A, editors. Cellular Metals: Manufacure, Properties and Applications, Berlin: MIT-Verlag; 2003, p. 463-68.

[15] Tan P, Reid S, Harrigan J, Zou Z, Li S. Dynamic compressive strength properties of aluminium foams. Part I—experimental data and observations. J Mech Phys Solids 2005; 53:2174-205.

[16] Zhao H, Elnasri I, Abdennadher S. An experimental study on the behaviour under impact loading of metallic cellular materials. Int J Mech Sci 2005; 47:757-74.

[17] Mukai T, Miyoshi T, Nakano S, Somekawa H, Higashi K. Compressive response of a closed-cell aluminium foam at high strain-rate. Scripta Mater 2006; 54:533-7.

[18] Peroni L, Avalle M, Peroni M. The mechanical behaviour of aluminium foam structures in different loading conditions. Int J Impact Eng 2008; 35:644-58.

[19] Kiernan S, Cui L, Gilchrist M. Propagation of a stress wave through a virtual functionally graded foam. Int J Non-Linear Mech 2009; 44:456-68.

[20] Pochhammer L. On the Propagation Velocities of Small Oscillations in an Unlimited Isotropic Circular Cylinder. J Reine Angew Math 1876; 81:324-36.

[21] Chree C. The Equations of an Isotropic Elastic Solid in Polar and Cylindrical Coordinates, Their Solutions and Applications. Trans Cambridge Phil Soc 1889; 14:250-369.

[22] Irausquín I. Mechanical characterization of metal foams and its application on energy absorption systems. Doctoral thesis, University Carlos III of Madrid; 2012.

[23] Abaqus Analysis User's Manual. Version 6.9-2. SIMULIA; 2009.

[24] Deshpande V, Fleck N. Isotropic constitutive models for metallic foams. J Mech Phys Solids 2000; 48:1253-83.

[25] Miyoshi T, Itoh M, Akiyama S, Kitahara A. ALPORAS Aluminum Foam: Production Process, Properties, and Applications. Adv Eng Mater 2000; 2:179-83.

[26] Chen W, Lu F, Frew D, Forrestal M. Dynamic Compression Testing of Soft Materials. J Appl Mech 2000; 69:214-23.

[27] Chen W, Zhang B, Forrestal M. A Split Hopkinson Bar Technique for Low impedance Materials. Exp Mech 1999; 39:81-5.

[28] Mukai T, Kanahashi K, Miyoshi T, Mabuchi M, Nieh T, Higashi K. Experimental Study of Energy Absorption in a Close-Celled Aluminium Foam Under Dynamic Loading. Scripta Mater 1999; 40:921-7.

[29] DYMAT Standardisation RE/002B/87. Dynamic compression testing using the split Hopkinson

bar pressure bar. 2nd Version. DYMAT; 1999

[30] Ferry J. Viscoelastic Properties of Polymers. New York: Wiley; 1961

[31] Arnold ND, Guenther AH. Experimental determination of ultrasonic wave velocities in plastics as functions of temperature. I. Common plastics and selected nose-cone materials, J Appl Polym Sci 1966; 10(5):731-43.

[32] Asay JR, Guenther AH. Experimental determination of ultrasonic wave velocities in plastics as functions of temperature. IV. Shear velocities in common plastics. J Appl Polym Sci 1967; 11(7):1087-100.

[33] Segreti M, Rusinek A, Klepaczko J. Experimental study on puncture of PMMA at low and high velocities, effect on the failure mode. Polym Test 2004; 23:703-18.

[34] Afifi H. Ultrasonic pulse echo studies of the physical properties of PMMA, PS, and PVC. Polym-Plast Technol 2003; 42(2):193-205.

[35] Wang L, Labibes K, Azari Z, Pluvinage G. Generalization of split Hopkinson bar technique to use viscoelastic bars. Int J Impact Eng 1994; 15(5):669-86.

[36] Lifshitz JM, Leber II. Data processing in the split Hopkinson pressure bar tests. Int J Impact Eng 1994; 15(6):723-33.

[37] Peroni M, Peroni L, Avalle M. High strain-rate compression test on metallic foam using a multiple pulse SHPB Apparatus. J Phys IV 2006; 134:609-16.

[38] Paul A, Ramamurty U. Strain rate sensitivity of a closed-cell aluminium foam. Mater Sci Eng 2000; A 281:1-7.

Tables Caption

Table 1. Product of the mechanical impedance by the cross section area, ZA, for the materials considered when manufacturing the bars and for the Alporas 10% foam.

Figures Caption

Fig. 1. Schematic representation of a conventional SHPB device.

Fig. 2. SHPB device with PMMA bars and striker: a) side view, b) contact between striker and input bar and velocity measurement system.

Fig. 3. Incident and reflected waves registered from an empty SHPB test performed at 1.5 bar.

Fig. 4. Attenuation coefficient, $\alpha(\omega)$, obtained from an empty SHPB test at 1.5 bar.

Fig. 5. Comparison between the incident wave and the sum of the reflected and transmitted waves on the Alporas 10%: a) uncorrected b) corrected with the propagation coefficient, $\gamma(\omega)$, obtained at 1.5 bar.

Fig. 6. Nominal stress-strain curves, σ_N-ε_N, obtained from the uncorrected registered waves and from the waves corrected with the propagation coefficient, $\gamma(\omega)$, obtained at 1.5 bar.

Fig. 7. Nominal stress-strain curves, σ_N-ε_N, obtained from two tests on the Alporas 10% at 700 s^{-1} and the corresponding average.

Fig. 8. Average nominal stress-strain curves, σ_N-ε_N, obtained from the tests of the Alporas 10% at different strain rates.

Fig. 9. Variation of the nominal stress, σ_N, with the strain rate, $\dot{\varepsilon}$, for nominal strains, ε_N, between 0.05 and 0.15, obtained from SHPB tests of the Alporas 10%.

Fig. 10. Variation of the plateau stress, σ_{pl}, compressive strength, σ_c, and yield stress at 0.2% strain, σ_y, with the strain rate, $\dot{\varepsilon}$, for SHPB tests of the Alporas 10%.

Fig. 11. Variation of the specific absorbed energy, W, with the strain rate, $\dot{\varepsilon}$, for nominal strains, ε_N, between 0.05 and 0.15, obtained from SHPB tests of the Alporas 10%.

Table 1.

Material	*Steel*	*PMMA*	*Nylon PA6*	*Alporas %*
ZA (kNs/m)	32.3	1.6	1.5	0.26

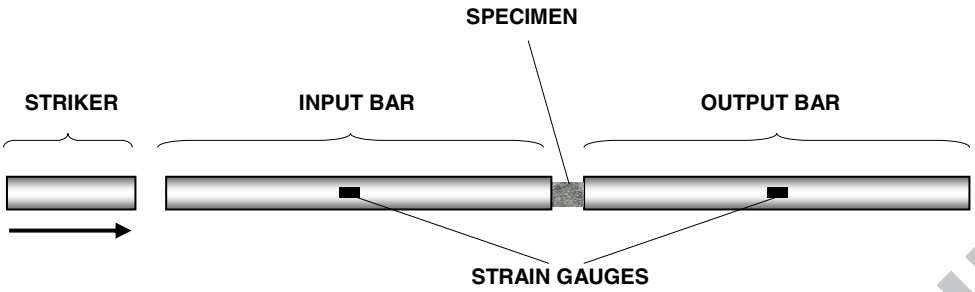

Fig. 1. Schematic representation of a conventional SHPB device.

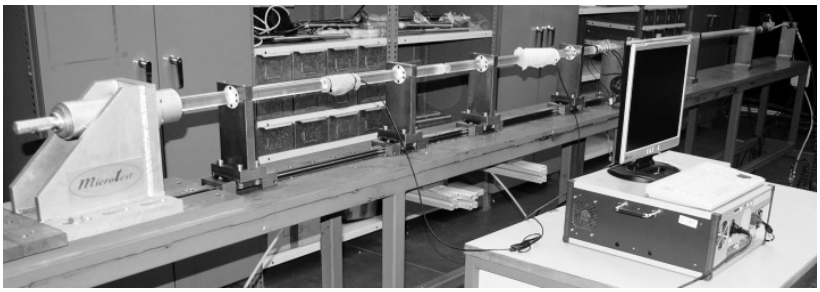

(a)

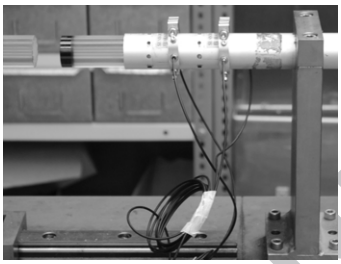

(b)

Fig. 2. SHPB device with PMMA bars and striker: a) side view, b) contact between striker and input bar and velocity measurement system.

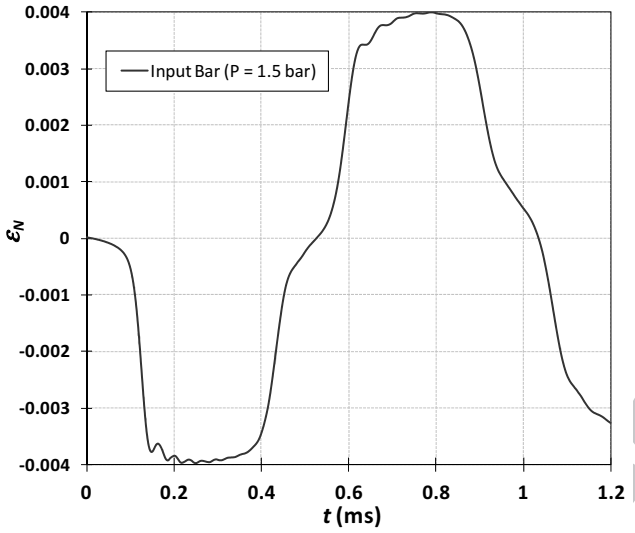

Fig. 3. Incident and reflected waves registered from an empty SHPB test performed at 1.5 bar.

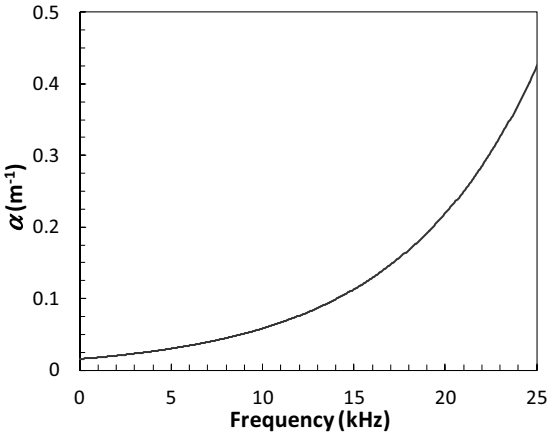

Fig. 4. Attenuation coefficient, $\alpha(\omega)$, obtained from an empty SHPB test at 1.5 bar.

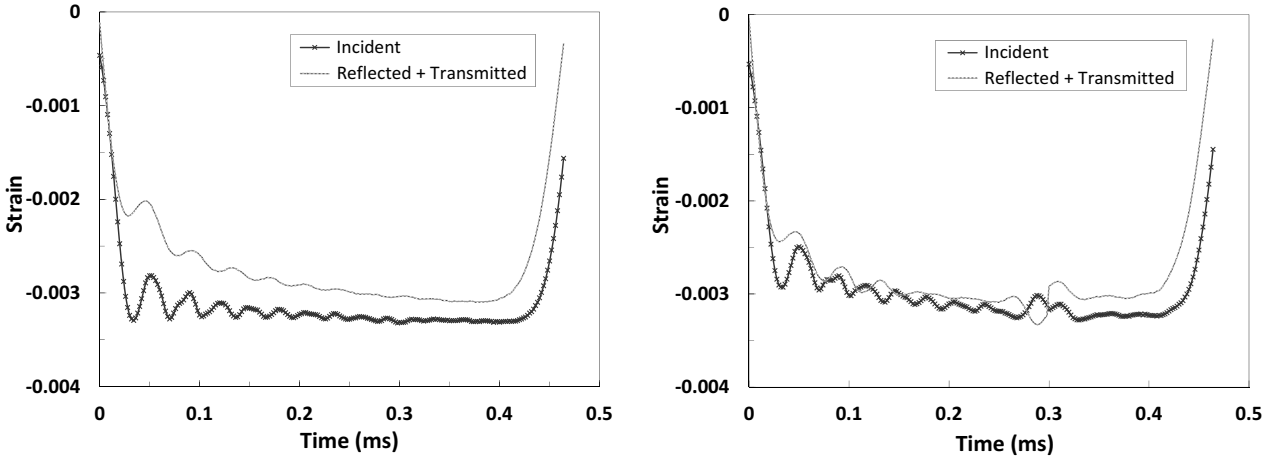

Fig. 5. Comparison between the incident wave and the sum of the reflected and transmitted waves on the Alporas 10%: a) uncorrected b) corrected with the propagation coefficient, $\gamma(\omega)$, obtained at 1.5 bar.

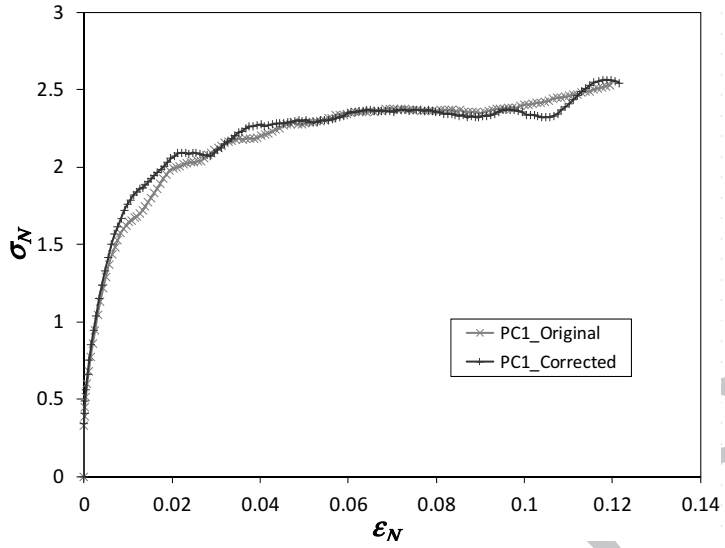

Fig. 6. Nominal stress-strain curves, σ_N-ε_N, obtained from the uncorrected registered waves and from the waves corrected with the propagation coefficient, $\gamma(\omega)$, obtained at 1.5 bar.

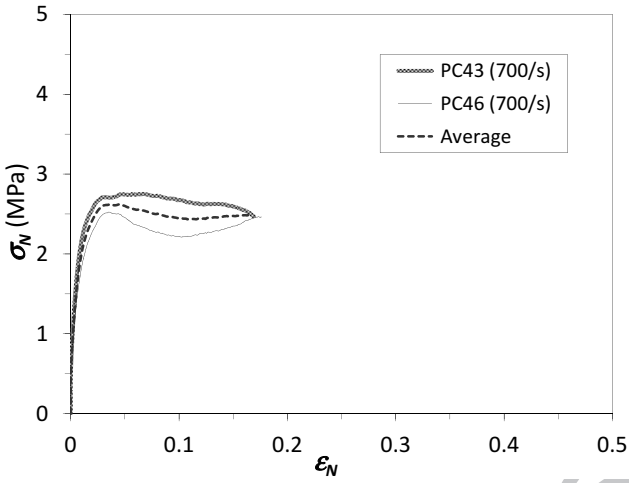

Fig. 7. Nominal stress-strain curves, σ_N-ε_N, obtained from two tests on the Alporas 10% at 700 s^{-1} and the corresponding average.

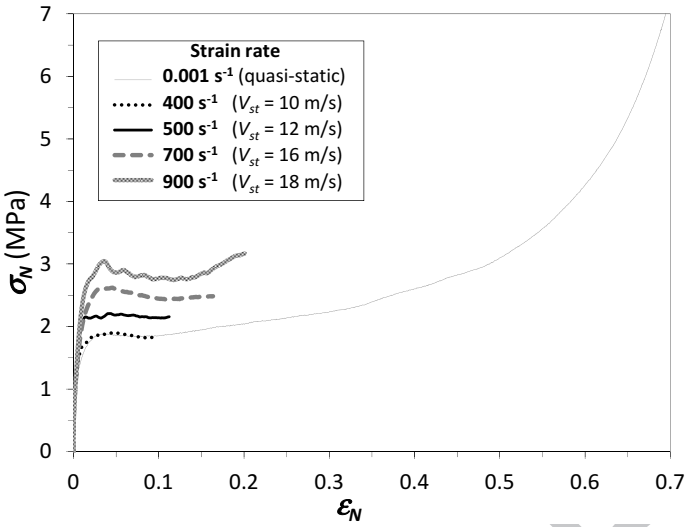

Fig. 8. Average nominal stress-strain curves, σ_N-ε_N, obtained from the tests of the Alporas 10% at different strain rates.

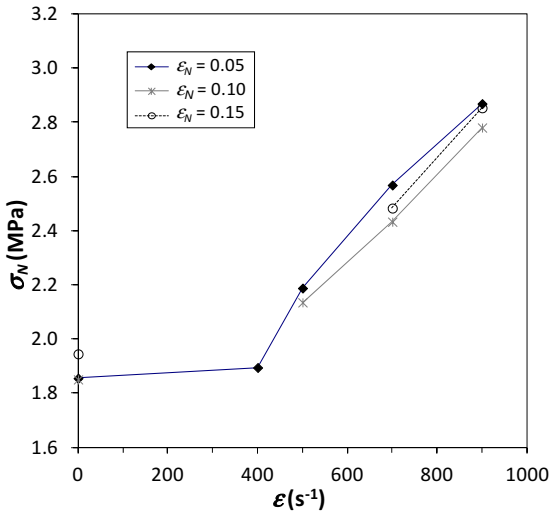

Fig. 9. Variation of the nominal stress, σ_N, with the strain rate, $\dot{\varepsilon}$, for nominal strains, ε_N, between 0.05 and 0.15, obtained from SHPB tests of the Alporas 10%.

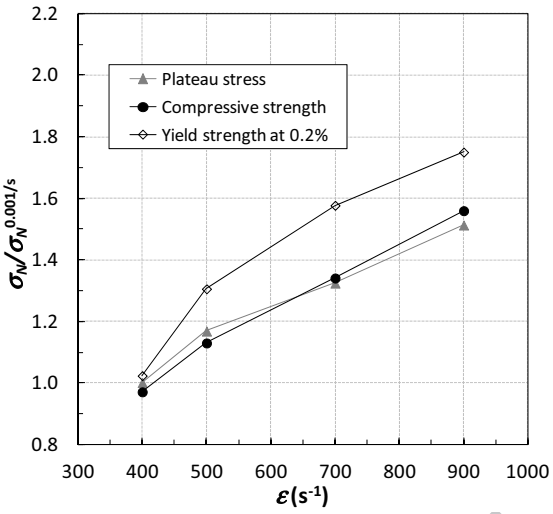

Fig. 10. Variation of the plateau stress, σ_{pl}, compressive strength, σ_c, and yield stress at 0.2% strain, σ_y, with the strain rate, $\dot{\varepsilon}$, for SHPB tests of the Alporas 10%.

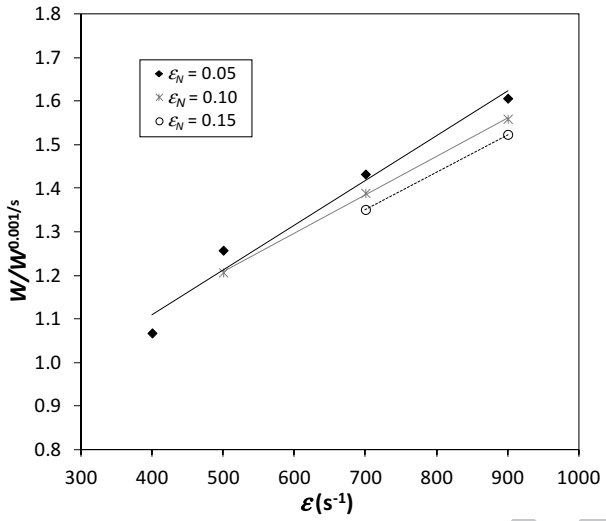

Fig. 11. Variation of the specific absorbed energy, W, with the strain rate, $\dot{\varepsilon}$, for nominal strains, ε_N, between 0.05 and 0.15, obtained from SHPB tests of the Alporas 10%.

Research Highlights

- PMMA has shown to be suitable material for the dynamic testing of the Alporas foam.
- A dynamic Young's modulus of the PMMA was estimated by an ultrasonic technique.
- Viscoelastic dispersion and attenuation effects due to the PMMA were corrected.
- We obtained the stress-strain curves of the Alporas foam at different strain rates.
- The mechanical properties of the Alporas foam exhibit some strain rate sensitivity.